

High mobility group box 1 in dilated cardiomyopathy. Kido et al. 1

1 The administration of high-mobility group box 1 fragment prevents deterioration of cardiac
2 performance by enhancement of bone marrow mesenchymal stem cell homing in the
3 delta-sarcoglycan-deficient hamster

4

5 Takashi Kido, MD, PhD¹, Shigeru Miyagawa, MD, PhD¹, Takasumi Goto, MD¹, Katsuto
6 Tamai, MD, PhD², Takayoshi Ueno, MD, PhD¹, Koichi Toda, MD, PhD¹, Toru Kuratani, MD,
7 PhD¹,
8 Yoshiki Sawa, MD, PhD¹*

9

10 ¹Department of Cardiovascular Surgery, Osaka University Graduate School of Medicine

11 ²Department of Stem Cell Therapy Science, Osaka University Graduate School of Medicine

12

13 *Corresponding Author

14 E-mail address: sawa-p@surg1.med.osaka-u.ac.jp

15

16 These authors contributed equally to this work.

17

18

19

20 **Abstract**

21 **Objectives:** We hypothesized that systemic administration of high-mobility group box 1
22 fragment attenuates the progression of myocardial fibrosis and cardiac dysfunction in a hamster
23 model of dilated cardiomyopathy by recruiting bone marrow mesenchymal stem cells thus
24 causing enhancement of a self-regeneration system.

25 **Methods:** Twenty-week-old J2N-k hamsters, which are δ -sarcoglycan-deficient, were treated
26 with systemic injection of high-mobility group box 1 fragment (HMGB1, n=15) or phosphate
27 buffered saline (control, n=11). Echocardiography for left ventricular function, cardiac
28 histology, and molecular biology were analyzed. The life-prolonging effect was assessed
29 separately using the HMGB1 and control groups, in addition to a monthly HMGB1 group which
30 received monthly systemic injections of high-mobility group box 1 fragment, 3 times (HMGB1,
31 n=11, control, n=9, monthly HMGB1, n=9).

32 **Results:** The HMGB1 group showed improved left ventricular ejection fraction, reduced
33 myocardial fibrosis, and increased capillary density. The number of platelet-derived growth
34 factor receptor-alpha and CD106 positive mesenchymal stem cells detected in the myocardium
35 was significantly increased, and intra-myocardial expression of tumor necrosis factor α
36 stimulating gene 6, hepatic growth factor, and vascular endothelial growth factor were

High mobility group box 1 in dilated cardiomyopathy. Kido et al. 3

37 significantly upregulated after high-mobility group box 1 fragment administration. Improved

38 survival was observed in the monthly HMGB1 group compared with the control group.

39 **Conclusions:** Systemic high-mobility group box 1 fragment administration attenuates the

40 progression of left ventricular remodeling in a hamster model of dilated cardiomyopathy by

41 enhanced homing of bone marrow mesenchymal stem cells into damaged myocardium,

42 suggesting that high-mobility group box 1 fragment could be a new treatment for dilated

43 cardiomyopathy.

44

45

46

47

48

49

50

51

52

53

54

55 **Introduction**

56 Dilated cardiomyopathy (DCM) is one of the most common causes of heart failure and is
57 associated with left ventricular dilatation and contractile dysfunction [1]. While significant
58 improvements have been made in medical therapies, such as angiotensin-converting enzyme
59 inhibitors and beta-blockers [2], and interventions, such as implantable cardioverter
60 defibrillators [3] and cardiac resynchronization therapy [4], the prognosis for heart failure
61 patients is still poor with 1-year mortality of 25–30% and a 50% survival rate at 5 years [5].
62 DCM remains the most common indication for cardiac transplantation but donor shortages have
63 become a serious issue. To deal with this problem, several novel approaches using cell therapy
64 have been developed in DCM patients with encouraging results [6–8].

65

66 Stem cells are an endogenous physiological healing mechanism of the body. A number of
67 reports have suggested that damaged tissues may release various cytokines, which facilitate not
68 only the mobilization of bone marrow-derived mesenchymal stem cells (BMMSCs) into the
69 peripheral blood, but also their homing to sites of wound healing [9–11]. The enhancement of
70 such healing mechanisms by drug administration might have beneficial effects in various
71 diseases.

72

High mobility group box 1 in dilated cardiomyopathy. Kido et al. 5

73 High-mobility group box 1 (HMGB1) is a non-histone nuclear protein that regulates chromatin
74 structure remodeling by acting as a molecular chaperone in the chromatin DNA-protein
75 complex [12]. Previous reports have demonstrated that endogenous platelet-derived growth
76 factor receptor-alpha positive (PDGFR α^+) BMMSCs accumulate in damaged tissue and
77 contribute to regeneration in response to elevated HMGB1 levels in serum [13]. Moreover,
78 systemic administration of HMGB1 further induces the accumulation of PDGFR α^+ BMMSCs in
79 the damaged tissue through CXCR4 upregulation, which is followed by significant
80 inflammatory suppression [14].

81
82 Since BMMSCs have been reported to have therapeutic effect in DCM through paracrine effects
83 [6,7], the above-mentioned “drug-induced endogenous regenerative therapy” might have
84 effectiveness for DCM without supply of viable ex vivo cells. Recently, we developed a
85 HMGB1 fragment containing the mesenchymal stem cell mobilization domain from human
86 HMGB1. We hypothesize that systemic administration of this HMGB1 fragment attenuates the
87 progression of myocardial fibrosis and cardiac dysfunction in a hamster model of DCM by
88 recruitment of BMMSCs, promoting self-regeneration.

89

90

91 **Material and Methods**

92 Animal procedures were carried out under the approval of the Institutional Ethics Committee

93 (reference number 28-011-002). The investigation conformed to the “Principles of Laboratory

94 Animal Care” formulated by the National Society for Medical Research and the “Guide for the

95 Care and Use of Laboratory Animals” (National Institutes of Health Publication). All

96 experimental procedures and evaluations were performed in a blinded manner.

97

98 *Experimental Animals*

99 Male J2N-k hamsters, which are deficient in δ -sarcoglycan, were used for this study. J2N-k

100 hamsters are an established animal model of DCM. They exhibit progressive myocardial

101 fibrosis and moderate cardiac dysfunction at 8–9 weeks of age. Accordingly, the average life

102 span of J2N-k hamsters is much shorter (approximately 42 weeks) than control hamsters

103 (approximately 112 weeks) [15,16].

104

105 *HMGB1 Fragment*

106 Mesenchymal stem cell mobilization domain from human HMGB1 was produced as “HMGB1

107 fragment” by solid-phase synthesis and provided by StemRIM (StemRIM Inc., Osaka, Japan).

108 The HMGB1 fragment was dissolved in phosphate buffered saline (PBS) to a concentration of 1
109 mg/ml before administration.

110

111 *Procedure of HMGB1 Fragment Administration*

112 Male 19-week-old J2N-k hamsters were purchased from Japan SLC (Shizuoka, Japan). HMGB1
113 fragment (3mg/kg/day; HMGB1, n= 15) or PBS (3ml/kg/day; control, n=11) was administered
114 for 4 consecutive days at the age of 20 weeks in the following manner: The external jugular vein
115 was exposed by a median neck skin incision under 1.5% isoflurane anesthesia. Subsequently,
116 HMGB1 fragment or PBS was injected through the external jugular vein. After the complete
117 hemostasis, the skin incision was closed, and the hamsters were housed in a
118 temperature-controlled cage.

119

120 *Transthoracic Echocardiography*

121 Transthoracic echocardiography was performed to assess cardiac function using M-mode
122 echocardiography with Vivid I (GE Healthcare) under isoflurane inhalation (1%). Diastolic and
123 systolic dimensions of the left ventricle (LVDd/Ds), and left ventricular ejection fraction
124 (LVEF) were measured before treatment, and reassessed at 4 and 6 weeks after treatment.

125

126 *Histological Analysis*

127 The heart was excised under isoflurane anesthesia (5%) 6 weeks after treatment to perform

128 histological and molecular biological analysis. The excised heart was fixed with either 10%

129 buffered formalin for paraffin sections or 4% paraformaldehyde for frozen sections. The

130 paraffin sections were stained with picrosirius red to assess the degree of myocardial fibrosis.

131 The paraffin sections were used for immunohistochemistry and labeled using polyclonal CD31

132 antibody (1:50 CD31, Abcam, Cambridge, UK), anti- α -sarcoglycan (clone: Ad1/20A6;

133 Novocastra, Weltzar, Germany), and anti- α -dystroglycan (clone: VIA4-1; Upstate

134 Biotechnology, Lake Placid, NY) to assess capillary vascular density and the organization of

135 cytoskeletal proteins. The paraffin sections were also labeled using rabbit monoclonal

136 anti-CD106 antibody (ab134047, Abcam, Cambridge, MA) and goat polyclonal anti-PDGFR α

137 (R&D). PDGFR α and CD106 are known to be expressed in BMMSCs and are commonly used

138 as markers for mesenchymal stem cells (MSCs) [17,18]. The frozen sections were also used for

139 immunohistochemistry and labeled with rabbit polyclonal anti-SDF1 antibody (ab9797, Abcam,

140 Cambridge, MA) and mouse monoclonal CXCR4 antibody (4G10, sc-53534, Santa Cruz

141 Biotechnology). The frozen sections were also stained with 4-hydroxynonenal to estimate lipid

142 peroxidation [19], and dihydroethidium to estimate superoxide production [20].

143

High mobility group box 1 in dilated cardiomyopathy. Kido et al. 9

144 More than 5 sections were prepared per specimen and 3 low power fields per section were
145 analyzed and averaged. The fibrotic area, the expression of α -sarcoglycan and α -dystroglycan,
146 and the 4-hydroxynonenal positive area were measured using Metamorph image analysis
147 software (Molecular Devices, Inc., Downingtown, PA). The capillary density, the number of
148 PDGFR α^+ and CD106 positive (CD106 $^+$) cells, the number of CXCR4 positive (CXCR4 $^+$) cells
149 and SDF-1 positive area (mm 2), and the number of dihydroethidium positive dots were
150 measured using the BZ-analysis software (Keyence, Tokyo, Japan).

151

152 *Transmission electron microscopy*

153 Cardiac tissue was pre-fixed with Karnovsky fixative containing 2.5% glutaraldehyde, 2%
154 paraformaldehyde in a 0.1 M (pH 7.4) cacodylate buffer for 2 hours at 4°C and post-fixed with
155 2% osmium tetroxide for 2 hours at 4°C. The samples were then immersed in 0.5% uranyl
156 acetate for 3 hours at room temperature, dehydrated in ethanol (50%, 70%, 80%, 90%, 95%, and
157 100%) and propylene oxide, and embedded in epoxy resin. Semithin sections (0.5 μ m) were
158 stained with 0.1% toluidine blue solution and examined under a light microscope. Ultrathin
159 sections were made with a Leica ultramicrotome. These sections were counterstained with
160 uranyl acetate and lead citrate, before examination with a Hitachi H-7100 electron microscope
161 at 75 kV.

162

163 *Real-Time Polymerase Chain Reaction*

164 Total RNA was extracted from cardiac tissue and reverse transcribed using Omniscript reverse

165 transcriptase (Qiagen, Hilden, Germany). The resulting cDNA was used for real-time

166 polymerase chain reaction with the ABI PRISM 7700 system (Applied Biosystems) and

167 Taqman Universal Master Mix (Applied Biosystems, Division of Life Technologies

168 Corporation, Carlsbad, Calif) and using hamster-specific primers for tumor necrosis factor- α

169 stimulating gene 6 (TSG-6), vascular endothelial growth factor (VEGF), and CXCR4. Each

170 sample was analyzed in duplicate for each gene studied. Data were normalized to

171 glyceraldehyde-3-phosphate dehydrogenase expression level. For relative expression analysis,

172 the ddCT method was used, and a sample from a control hamster was used as reference. The

173 real-time polymerase reaction was also conducted using Fast SYBR Green Master Mix and

174 primers designed for hepatic growth factor and glyceraldehyde-3-phosphate dehydrogenase as

175 shown in Table 1. For relative expression analysis, we prepared a 5-fold serial standard curve

176 using a sample from a HMGB1 hamster as reference.

177 Table 1. Forward and reverse primers and probe

| | F-primer | R-primer | Probe |
|-------|-----------------------------|-------------------------------|-------------------------------|
| GAPDH | CTG CAC CAC CAC CTG CTT AGC | GCC ATG CCA GTG AGC TTC C | CTG CAC CAC CAC CTG CTT AGC |
| HGF | AGG TCC CAT GGA TCA CAC AGA | GCC CTT GTC GGG ATA TCT TTC T | ACC AGC AGA CAC CAC ACC GGC A |

182 GAPDH, glyceraldehyde-3-phosphate dehydrogenase; HGF, hepatic growth factor

183 *Evaluation of hamster prognosis after treatment*

184 The life-prolonging effect of the HMGB1 fragment on J2N-k hamsters was assessed separately.

185 Twenty-week-old J2N-k hamsters were treated with HMGB1 (HMGB1, n= 11) or PBS (control,

186 n= 9) as described above. An additional treatment group received monthly administration of

187 HMGB1 fragment 3 times, (monthly HMGB1, n= 9) to evaluate the long-term therapeutic

188 effects of HMGB1 fragment (Fig 1). The animals were randomly allocated to each treatment

189 group and housed after the initial treatment. The survival rate in the 3 groups was calculated by

190 the Kaplan–Meier method using JMP Pro 12 (SAS Institute, Cary, NC, USA) and the

191 significant difference between the groups was tested at 22 weeks (equal to 42 weeks of age, the

192 average lifespan of J2N-k hamsters) by log-rank analysis.

193

194 *Statistical Analysis*

195 Continuous variables were summarized as means with standard deviations and compared using

196 an unpaired t-test. Survival curves were prepared using the Kaplan–Meier method and

197 compared using the log-rank test. All data were analyzed using JMP Pro 12. Differences were

198 considered statistically significant at P-values < 0.05.

199

200 **Results**

201 *Preserved Cardiac Performance with HMGB1 Fragment Administration*

202 The functional effects of HMGB1 fragment on the DCM heart were assessed by transthoracic

203 echocardiography over time. LVDd/Ds and LVEF at 20 weeks of age, just before the treatment,

204 were not significantly different between the HMGB1 group and the control group. After

205 treatment, echocardiography showed that the LVEF was significantly preserved until 6 weeks in

206 the HMGB1 group compared with the control group (4 weeks: $43\pm8\%$ vs $33\pm9\%$, $p=0.01$; 6

207 weeks: $41\pm7\%$ vs $31\pm7\%$, $p=0.0001$, HMGB1 vs control, respectively) (Fig 1).

208

209 **Fig 1.**

210 Changes in LVEF (a), LVDd (b), and LVDs (c) over time after the treatment.

211 Diastolic and systolic dimensions of the left ventricle, and LVEF were measured before

212 treatment, and reassessed at 4 and 6 weeks after treatment. The LVEF was significantly

213 preserved until 6 weeks after the treatment in the HMGB1 group compared with the control

214 group.

215 LVEF, left ventricular ejection fraction; LVDd, left ventricular diastolic dimension; LVDs, left

216 ventricular systolic dimension.

217

218 *Effect of HMGB1 Fragment on Myocardial Fibrosis*

219 The degree of myocardial fibrosis 6 weeks after HMGB1 fragment treatment was assessed by

220 picrosirius red staining and compared with control group. Quantification of fibrotic area

221 confirmed that the degree of myocardial fibrosis was significantly reduced in the HMGB1 group

222 compared with the control group (16.6±3.8% vs 22.7±5.4%, respectively, p=0.04) (Fig 2).

223

224 **Fig 2.**

225 Suppression of myocardial fibrotic change in J2N-k hamsters by HMGB1 fragment.

226 (a), Representative photomicrographs (×20, scale bar=1000μm) of picrosirius red staining.

227 (b), Tissue sections were stained by picrosirius red and the fibrous area was quantified by image

228 analysis. Percentage of myocardial fibrosis was significantly less in the HMGB1 group than in

229 the control group.

230 HMGB1, high-mobility group box 1.

231

232 *Increased Vasculature in the Heart After HMGB1 Fragment Administration*

233 Capillary vascular densities 6 weeks after the treatment were assessed by CD31

234 immunostaining. In the HMGB1 group, the number of CD31 positive arterioles and capillaries

High mobility group box 1 in dilated cardiomyopathy. Kido et al. 15

235 was significantly increased compared with the control group (654 ± 171 units/mm² vs 484 ± 74
236 units/mm², respectively, $p=0.02$) (Fig 3).

237

238 **Fig 3.**

239 Increased myocardial capillary density in J2N-k hamsters by HMGB1 fragment.

240 (a), Representative photomicrographs ($\times 200$, scale bar= $50\mu\text{m}$) of anti-CD31 staining.

241 (b), Tissue sections were immunostained for CD31 and the capillary density was measured with
242 the analysis software. The HMGB1 group showed significantly higher capillary vascular density
243 than the control group.

244 HMGB1, high-mobility group box 1.

245

246 *PDGFR α and CD106 Positive Cells in the Hearts*

247 Immunohistochemistry showed that the number of PDGFR α^+ and CD106 $^+$ cells in the heart
248 tissue was significantly greater in HMGB1 group compared with the control group (12 ± 5 cells
249 /field vs 4 ± 2 cells/field, respectively, $p<0.001$) (Fig 4).

250

251 **Fig 4.**

High mobility group box 1 in dilated cardiomyopathy. Kido et al. 16

252 The increased accumulation of PDGFR α^+ and CD106 $^+$ cells in the heart tissue by HMGB1

253 fragment.

254 (a), Representative photomicrographs ($\times 1000$, scale bar=50 μm) of PDGFR α (green), CD106

255 (red) staining.

256 (b), Tissue sections were immunostained for PDGFR α and CD106. The number of PDGFR α^+

257 and CD106 $^+$ cells was measured with the analysis software. The HMGB1 group showed

258 significantly increased numbers of PDGFR α^+ and CD106 $^+$ cells than the control group.

259 PDGFR α , platelet-derived growth factor receptor-alpha; HMGB1, high-mobility group box 1.

260

261 *Increased CXCR4 Positive Cells in the Heart after HMGB1 Fragment Administration*

262 Immunohistochemistry showed significantly increased ratio of the number of CXCR4 $^+$ cells to

263 SDF-1 positive area (mm^2) in heart tissue in the HMGB1 group than in the control group

264 (1.3 \pm 1.0 vs 0.3 \pm 0.1 cells/ mm^2 , respectively, $p=0.02$) (Fig 5).

265

266 **Fig 5.**

267 Increased CXCR4 $^+$ cells in SDF-1 positive area in the heart tissue by HMGB1 fragment.

268

High mobility group box 1 in dilated cardiomyopathy. Kido et al. 17

269 (a), Representative photomicrographs ($\times 600$, scale bar=50 μ m) of SDF-1 (green) and CXCR4

270 (red) staining.

271 (b), Tissue sections were immunostained for CXCR4 and SDF-1. The number of CXCR4 $^{+}$ cells

272 was measured with analysis software and SDF-1 positive area was measured with image

273 analysis. The HMGB1 group showed significantly higher CXCR4 $^{+}$ cells to SDF-1 positive area

274 (mm^2) in heart tissue than the control group.

275 HMGB1, high-mobility group box 1; SDF-1, stromal derived factor-1.

276

277 *Preservation of Cytoskeletal Proteins after HMGB1 Fragment Administration*

278 Immunohistochemistry showed increased expression of α -sarcoglycan and α -dystroglycan in the

279 basement membrane beneath the cardiomyocytes in HMGB1 group, whereas lower expression

280 levels of these proteins was seen in the control group (α -sarcoglycan, $12.2 \pm 2.7\%$ vs $2.8 \pm 1.4\%$,

281 $p < 0.001$, α -dystroglycan, $20.2 \pm 3.5\%$ vs $8.3 \pm 1.8\%$, $p < 0.001$, HMGB1 vs control, respectively)

282 (Fig 6).

283

284 **Fig 6.**

285 Immunostaining for alpha-sarcoglycan and alpha-dystroglycan in cardiomyocytes.

High mobility group box 1 in dilated cardiomyopathy. Kido et al. 18

286 (a), Representative photomicrographs ($\times 600$, scale bar=50 μ m) of immunostaining of
287 α -sarcoglycan and α -dystroglycan in cardiomyocytes.
288 (b), Quantitative analysis of immunohistologic signals showed significantly increased staining
289 of both α -sarcoglycan and α -dystroglycan in HMGB1 group than the control group.
290 HMGB1, high-mobility group box 1.

291

292 *Mitochondrial Ultramicrostructure*

293 Transmission electron microscopy of the myocardium showed a relatively regular arrangement
294 of mitochondrial cristae in the HMGB1 group. In contrast, the mitochondrial cristae were
295 disordered in the control group (Fig 7).

296

297 **Fig 7.**

298 Mitochondrial ultramicrostructure was detected by TEM. Representative image ($\times 12000$) of
299 mitochondrial morphology and cristae of myocardium in the HMGB1 group and the control
300 group. The HMGB1 group showed relatively regular arrangement of mitochondrial cristae
301 compared with the control group.

302 TEM, Transmission electron microscopy; HMGB1, high-mobility group box 1.

303

304 *Effect of HMGB1 Fragment on Oxidative Stress in the Hearts*

305 The lipid peroxidation and superoxide production were assessed by 4-hydroxynonenal staining

306 and dihydroethidium staining, respectively. The results showed a trend towards reduced lipid

307 peroxidation ($3.5\pm2.4\%$ vs $5.6\pm3.7\%$, $p=0.06$, HMGB1 vs control) and a significant reduction

308 in superoxide production in the HMGB1 group compared with control (219 ± 32 units/mm 2 vs

309 1185 ± 97 units/mm 2 , respectively, $p<0.0001$) (Fig 8).

310

311 **Fig 8.**

312 Decreased oxidative stress in the heart tissue by HMGB1 fragment.

313 Representative photomicrographs of dihydroethidium staining ($\times 400$, scale bar= $50\mu\text{m}$) (a) and

314 4-hydroxynonenal staining ($\times 100$, scale bar= $50\mu\text{m}$) (b).

315 Tissue sections were stained with dihydroethidium to estimate superoxide production, and

316 4-hydroxynonenal to estimate lipid peroxidation. The HMGB1 group showed significantly

317 reduced production of superoxide (c) and a trend towards reduced lipid peroxidation (d)

318 compared with the control group.

319 HMGB1, high-mobility group box 1.

320

321 *Upregulated TSG-6, VEGF, HGF, and CXCR4 in the Heart after HMGB1 Fragment*

322 *Administration*

323 Real-time PCR was used to quantitatively assess the expression levels of BMMSC-derived

324 factors, such as VEGF, TSG-6, HGF, and CXCR4. Intramyocardial mRNA levels of VEGF,

325 TSG-6, and HGF were significantly upregulated in HMGB1 group compared with the control

326 group (TSG-6, 1.5 ± 0.6 vs 1.1 ± 0.2 , $p = 0.03$, VEGF, 1.3 ± 0.4 vs 1.0 ± 0.2 , $p = 0.04$, HGF, 3.2 ± 2.3

327 vs 1.3 ± 0.6 , $p = 0.02$, HMGB1 vs control, respectively). The intramyocardial mRNA levels of

328 CXCR4 in the HMGB1 group showed a trend towards increased expression compared with

329 control (1.5 ± 0.4 vs 1.2 ± 0.3 , respectively, $p = 0.06$).

330

331 *Survival Benefit of Monthly HMGB1 Administration*

332 Survival of J2N-k hamsters was assessed using the Kaplan–Meier method. There was no

333 significant difference in survival between HMGB1 and control. In contrast, the monthly

334 HMGB1 group all survived to the full 42 weeks, and they showed significantly improved

335 survival rate compared with control group (log-rank $p = 0.001$) (Fig 9).

336

337 **Fig 9.**

338 Survival after each treatment assessed by the Kaplan–Meier method.

339 There was no significant difference between the single HMGB1 treatment (n=11) group and the
340 control group (n=9), whereas the monthly HMGB1 group (n=9) showed a significantly greater
341 survival rate than control (p=0.01).

342

343 **Discussion**

344 In the present study we have shown that, first, systemic administration of HMGB1 fragment
345 leads to the accumulation of PDGFR α^+ and CD106 $^+$ cells in damaged myocardium possibly
346 through the SDF-1/CXCR4 axis and upregulated expression of cardioprotective factors such as
347 TSG-6, VEGF, and HGF in the heart tissue of J2N-k hamsters. Second, the myocardial
348 histology in the HMGB1 group demonstrated significantly decreased fibrosis, increased
349 capillary vascular density, decreased oxidative stress, and well-organized cytoskeletal proteins
350 compared with the control group. Finally, cardiac function was significantly preserved after
351 HMGB1 fragment administration and the survival benefit was shown with monthly HMGB1
352 fragment treatment.

353

354 The present study demonstrates the feasibility of “drug-induced endogenous regenerative
355 therapy” using an HMGB1 fragment in a hamster model of DCM . While the precise
356 mechanism remains unclear, it is well known that HMGB1 acts as a chemoattractant for MSCs
357 [13,14,21]. Systemic HMGB1 administration has been reported to induce accumulation of
358 PDGFR α^+ cells around blood vessels in the bone marrow and significant increases in these cells
359 in the peripheral blood [13]. In addition, the enhancement of CXCR4 expression with HMGB1

360 treatment promotes the local migration to damaged tissue through the SDF-1/CXCR4 axis,

361 which might be essential in DCM [22] as well as ischemic cardiomyopathy [23–25].

362

363 While PDGFR α^+ BMMSCs might be the predominant cell population mobilized by

364 administration of HMGB1 fragment and therefore exerting therapeutic effects on damaged

365 myocardium, it has been suggested that PDGFR α^+ MSCs include other defined subpopulations

366 with distinct functions [26]. As HMGB1 is also reported to induce other cell types [27], the

367 accumulated cells in damaged heart tissue after HMGB1 administration might be highly

368 heterogeneous and it will therefore be important to identify in the future, specific PDGFR α^+

369 subpopulations induced by HMGB1 which have therapeutic benefits.

370

371 Paracrine signaling is a well-investigated mechanism of protective effects exhibited by

372 BMMSCs on surrounding cells [28–32]. TSG-6 plays a key role in the anti-inflammatory effects

373 of BMMSCs [31,33]. TSG-6 attenuates oxidative stress through activation of CD44 [34,35], and

374 downregulates TGF- β by suppressing plasmin activity [33], which could result in decreased

375 myocardial fibrosis. Since increased oxidative stress is one of the essential factors in the

376 pathogenesis of myocardial fibrotic changes in J2N-k hamsters [16], our results suggest that

377 HMGB1 fragment administration could become a substantial therapy for DCM. VEGF has been

378 known to promote angiogenesis in ischemic conditions [29,36,37], which might have a
379 beneficial effect on the defective vascularization within the left ventricle, which is associated
380 with the pathophysiology of DCM [38,39]. HGF is known to be a putative paracrine mediator in
381 cardiac repair mechanisms of BMMSCs [40]. Our group has previously reported that HGF
382 induced the appropriate microenvironment for extracellular matrix remodeling, including strong
383 expression of cytoskeletal proteins in damaged myocardium [41,42].

384

385 No significant difference in survival was observed between the HMGB1 and control groups,
386 however, animals that received monthly HMGB1 treatment showed significantly better survival
387 compared with control. The therapeutic benefits of HMGB1 fragment might be sustained by
388 repeated administration in J2N-k hamsters and further investigation concerning the optimal dose
389 and interval of administration of HMGB1 fragment will be needed for the clinical use of
390 HMGB1 fragment in DCM patients.

391

392

393

394

395

396 **Conclusion**

397 Systemic HMGB1 fragment administration attenuates the progression of left ventricular
398 remodeling in a hamster model of DCM by enhanced homing of BMMSCs into damaged
399 myocardium, suggesting that HMGB1 fragment could be beneficial in the treatment of DCM.

400

401

402

403

404

405

406

407

408

409

410

411

412

413

414 **Acknowledgments**

415 We thank Hanne Gadeberg, PhD, from Edanz Group (www.edanzediting.com/ac) for editing a

416 draft of this manuscript.

417

418

419

420

421

422

423

424

425

426

427

428

429

430

431

432 **Reference**

433 1. Weintraub RG, Semsarian C, Macdonald P. Dilated cardiomyopathy. *Lancet*.
434 2017;390:400-414.

435 2. Hoshikawa E, Matsumura Y, Kubo T, Okawa M, Yamasaki N, Kitaoka H, et al. Effect of
436 Left Ventricular Reverse Remodeling on Long-Term Prognosis After Therapy With
437 Angiotensin-Converting Enzyme Inhibitors or Angiotensin II Receptor Blockers and β
438 blockers in Patients With Idiopathic Dilated Cardiomyopathy. *Am J Cardiol*.
439 2011;107:1065-1070

440 3. Kober L, Thune JJ, Nielsen JC, Haarbo J, Videbaek L, Kroup E, et al. Defibrillator
441 Implantation in Patients with Nonischemic Systolic Heart Failure. *N Engl J Med*.
442 2016;375:1221-1230

443 4. Ito M, Shinke T, Yoshida A, Kozuki A, Takei A, Fukuzawa K, et al. Reduction in coronary
444 microvascular resistance thorough cardiac resynchronization and its impact on chronic
445 reverse remodeling of left ventricle in patients with non-ischemic cardiomyopathy.
446 *Europace*. 2015;17:1407-1414

447 5. Dec GW, Fuster V. Idiopathic Dilated Cardiomyopathy. *N Engl J Med*.
448 1994;331:1564-1575

449 6. Fischer-Rasokat U, Assmus B, Seeger FH, Honold J, Leistner D, Fichtlscherer S, et al. A
450 Pilot Trial to Assess Potential Effects of Selective Intracoronary Bone Marrow-Derived
451 Progenitor Cell Infusion in Patients With Nonischemic Dilated Cardiomyopathy. *Circ Heart
452 Fail.* 2009;2:417-423

453 7. Bhargava B, Narang R, Ray R, Mohanty S, Gulati G, Kumar L, et al. The ABCD
454 (Autologous Bone Marrow Cells in Dilated Cardiomyopathy) Trial A Long-Term
455 Follow-Up Study. *J Am Coll Cardiol.* 2010;55:1643-1647

456 8. Vrtovec B, Poglajen G, Lezaic L, Sever M, Domanovic D, Cernelc P, et al. Effects of
457 Intracoronary CD34⁺ Stem Cell Transplantation in Nonischemic Dilated Cardiomyopathy
458 Patients. *Circ Res.* 2013;112:165-173

459 9. Chen Y, Xiang LX, Shao JZ, Pan RL, Wang YX, Dong XJ, et al. Recruitment of
460 endogenous bone marrow mesenchymal stem cells towards injured liver. *J Cell Mol Med.*
461 2010;14:1494-1508

462 10. Chen Y, Shao JZ, Xiang LX, Dong XJ, Zhang GR. Mesenchymal stem cells: A promising
463 candidate in regenerative medicine. *Int J Biochem Cell Biol.* 2008;40:815-820

464 11. Sasaki M, Abe R, Fujita Y, Ando S, Inokuma D, Shimizu H. Mesenchymal stem cells are
465 recruited into wounded skin and contribute to wound repair by transdifferentiation into
466 multiple skin cell type. *J Immunol.* 2008;15:2581-2587

467 12. Osmanov T, Ugrinova I, Pasheva E. The chaperone like function of the nonhistone protein

468 HMGB1. *Biochem Biophys Res Commun.* 2013;8:231-235

469 13. Tamai K, Yamazaki T, Chino T, Ishii M, Otsuru S, Kikuchi Y, et al. PDGFR α -positive cells

470 in bone marrow are mobilized by high mobility group box 1 (HMGB1) to regenerate injured

471 epithelia. *Proc Natl Acad Sci.* 2011;108:6609-6614

472 14. Aikawa E, Fujita R, Kikuchi Y, Kaneda Y, Tamai K. Systemic high-mobility group box 1

473 administration suppresses sakin inflammation by inducing an accumulation of PDGFR $^+$

474 mesenchymal cells from bone marrow. *Sci Rep.* 2015 Jun

475 5;5:11008.doi:10.1038/srep11008.

476 15. Mitsuhashi S, Saito N, Watano K, Igarashi K, Tagami S, Shima H, et al. Defect of

477 Delta-Sarcoglycan Gene Is Responsible for Development of Dilated Cardiomyopathy of a

478 Novel Hamster Strain, J2N-k: Calcineurin/PP2B Activity in the Heart of J2N-k Hamster. *J*

479 *Biochem* 2003;134:269-276

480 16. Maekawa K, Hirayama A, Iwata Y, Tajima Y, Nishimaki-Mogami T, Sugawara S, et al.

481 Global metabolic analysis of heart tissue in a hamster model for dilated cardiomyopathy. *J*

482 *Mol Cell Cardiol.* 2013 Jun;59:76-85. doi: 10.1016/j.yjmcc.2013.02.008.

483 17. Chamberlain G, Fox J, Ashton B, Middleton J. Concise Review: Mesenchymal Stem Cells:
484 Their Phenotype, Differentiation Capacity, Immunological Features, and Potential for
485 Homing. *Stem Cells*. 2007;25:2739-2749

486 18. Miwa H, Era T. Tracing the destiny of mesenchymal stem cells from embryo to adult bone
487 marrow and white adipose tissue via Pdgfra expression. *Development*. 2018 Jan 29;145(2).
488 pii: dev155879. doi: 10.1242/dev.155879.

489 19. Nakamura K, Kusano K, Nakamura Y, Kakishita M, Ohta K, Nagase S, et al. Carvedilol
490 Decreases Elevated Oxidative Stress in Human Failing Myocardium. *Circulation*.
491 2002;105:2867-2871

492 20. Fujii T, Onohara N, Maruyama Y, Tanabe S, Kobayashi H, Fukutomi M, et al.
493 Galphai2/13-mediated production of reactive oxygen species is critical for angiotensin
494 receptor-induced NFAT activation in cardiac fibroblasts. *J Bio Chem*. 2005;280:23041-7

495 21. Meng E, Guo Z, Wang H, Jin J, Wang J, Wang H, et al. High Mobility Group Box 1 Protein
496 Inhibits the Proliferation of Human Mesenchymal Stem Cells and Promotes Their Migration
497 and Differentiation along Osteoblastic Pathway. *Stem Cells Dev*. 2008;17:805-814

498 22. Theiss HD, David R, Engelmann MG, Barth A, Schotten K, Naebauer M, et al. Circulation
499 of CD34⁺ progenitor cell populations in patients with idiopathic dilated and ischemic
500 cardiomyopathy (DCM and ICM). *Eur Heart J*. 2007;28:1258-1264

501 23. Abbott JD, Huang Y, Liu D, Hickey R, Krause DS, Giordano FJ. Stromal Cell-Derived

502 Factor-1 α Plays a Critical Role in Stem Cell Recruitment to the Heart After Myocardial

503 Infaction but Is Not Sufficient to Induce Homing in the Absence of Injury. *Circulation*.

504 2004;110:3300-3305

505 24. Askari AT, Unzek S, Popovic ZB, Goldman CK, Forudi F, Kiedrowski M, et al. Effect of

506 stromal –cell-derived factor 1 on stem-cell homing and tissue regeneration in ischemic

507 cardiomyopathy. *Lancet* 2003;362:697-703

508 25. Hu X, Dai S, Wu WJ, Tan W, Zhu X, Mu J, et al. Stromal cell derived factor-1 alpha

509 confers protection against myocardial ischemia/reperfusion injury: role of the cardiac

510 stromal cell derived factor-1 alpha CXCR4 axis. *Circulation*. 2007;116:654-663

511 26. Jiang Y, Jahagirdar BN, Reinhardt RL, Schwartz RE, Keene CD, Ortiz-Gonzalez XR, et al.

512 Pluriotency of mesenchymal stem cells derived from adult marrow. *Nature* 2002;418:41-49

513 27. Palumbo R, Sampaolesi M, De Marchis F, Tonlorenzi R, Colombetti S, Mondino A, et al. *J*

514 *Cell Biol.* 2004;164:441-449

515 28. Uemura R, Xu M, Ahmad N, Ashraf M. Bone marrow stem cells prevent left ventricular

516 remodeling of ischemic heart through paracrine signaling. *Circ Res*. 2006;98:1414-1421

517 29. Markel TA, Wang Y, Herrmann JL, Crisostomo PR, Wang M, Novotny NM, et al. VEGF is

518 critical for stem cell-mediated cardioprotection and a crucial paracrine factor for defining

519 the age threshold in adult and neonatal stem cell function. Am J Physiol Hear Circ Physiol.

520 2008; 295:H2308-H2314

521 30. Kawamura M, Miyagawa S, Fukushima S, Saito A, Toda K, Daimon T, et al.

522 Xenotransplantation of Bone Marrow-Derived Human Mesenchymal Stem Cell Sheets

523 Attenuates Left Ventricular Remodeling in a Porcine Ischemic Cardiomyopathy Model.

524 Tissue Eng Part A. 2015;21:2272-2280

525 31. Lee RH, Yu JM, Peltier G, Reneau JC, Bazhanov N, Oh JY, et al. TSG-6 as a biomarker to

526 predict efficacy of human mesenchymal stem/progenitor cells in modulating sterile

527 inflammation in vivo. Proc Natl Acad Sci U S A. 2014;111:16766-71

528 32. Choi H, Lee RH, Bazhanov N, Oh JY, Prockop DJ. Anti-inflammatory protein TSG-6

529 secreted by activated MSCs attenuates zymosan-induced mouse peritonitis by decreasing

530 TLR2/NF-κB signaling in resident macrophages. Blood. 2011;118:330-338

531 33. Lee RH, Pulin AA, Seo MJ, Kota DJ, Ylostalo J, Larson BL, et al. Intravenous hMSCs

532 improve myocardial infarction in mice because cells embolized in lung are activated to

533 secrete the anti-inflammatory protein TSG-6. Cell Stem Cell 2009;5:54-63

534 34. Kota DJ, Wiggins LL, Yoon N, Lee RH. TSG-6 produced by hMSCs delays the onset of

535 autoimmune diabetes by suppressing Th1 development and enhancing tolerogenicity.

536 Diabetes. 2013;62:2048-2058

537 35. He Z, Hua J, Qian D, Gong J, Lin S, Xu C, et al. Intravenous hMSCs Ameliorate Acute
538 Pancreatitis in Mice via Secretion of Tumor Necrosis Factor- α Stimulated Gene/Protein 6.
539 Sci Rep. 2016 Dec 5;6:38438. doi: 10.1038/srep38438.
540 36. Neufeld G, Cohen T, Gengrinovitch S, Poltorak Z. Vascular endothelial growth factor
541 (VEGF) and its receptors. FASEB J. 1999;13:9-22
542 37. Zisa D, Shabbir A, Mastri M, Suzuki G, Lee T. Intramuscular VEGF repairs the failing
543 heart: role of host-derived growth factors and mobilization of progenitor cells. Am J Physiol
544 Regul Integr Comp Physiol. 2009;297:R1503-15
545 38. Roura S, Planas F, Prat-Vidal C, Leta R, Soler-Botija C, Carreras F, et al. Idiopathic dilated
546 cardiomyopathy exhibits defective vascularization and vessel formation. Eur J Heart Fail.
547 2007;9:995-1002
548 39. Mela T, Meyer TE, Pape LA, Chung ES, Aurigemma GP, Weiner BH. Coronary arterial
549 dimension-to-left ventricular mass ratio in idiopathic dilated cardiomyopathy. Am J Cardiol.
550 1999;83:1277-1280
551 40. Shafei AE, Ali MA, Ghanem HG, Shehata AI, Abdelgawad AA, Handal HR, et al.
552 Mechanistic effects of mesenchymal and hematopoietic stem cells: New therapeutic targets
553 in myocardial infarction. J Cell Biochem 2018;119:5274-5286

554 41. Miyagawa S, Sawa Y, Taketani S, Kawaguchi N, Nakamura T, Matsuura N, et al.

555 Myocardial regeneration therapy for heart failure: hepatocyte growth factor enhances the

556 effect of cellular cardiomyoplasty. 2002;105:2556-2561

557 42. Kondoh H, Sawa Y, Fukushima N, Matsumiya G, Miyagawa S, Kitagawa-Sakakida S, et al.

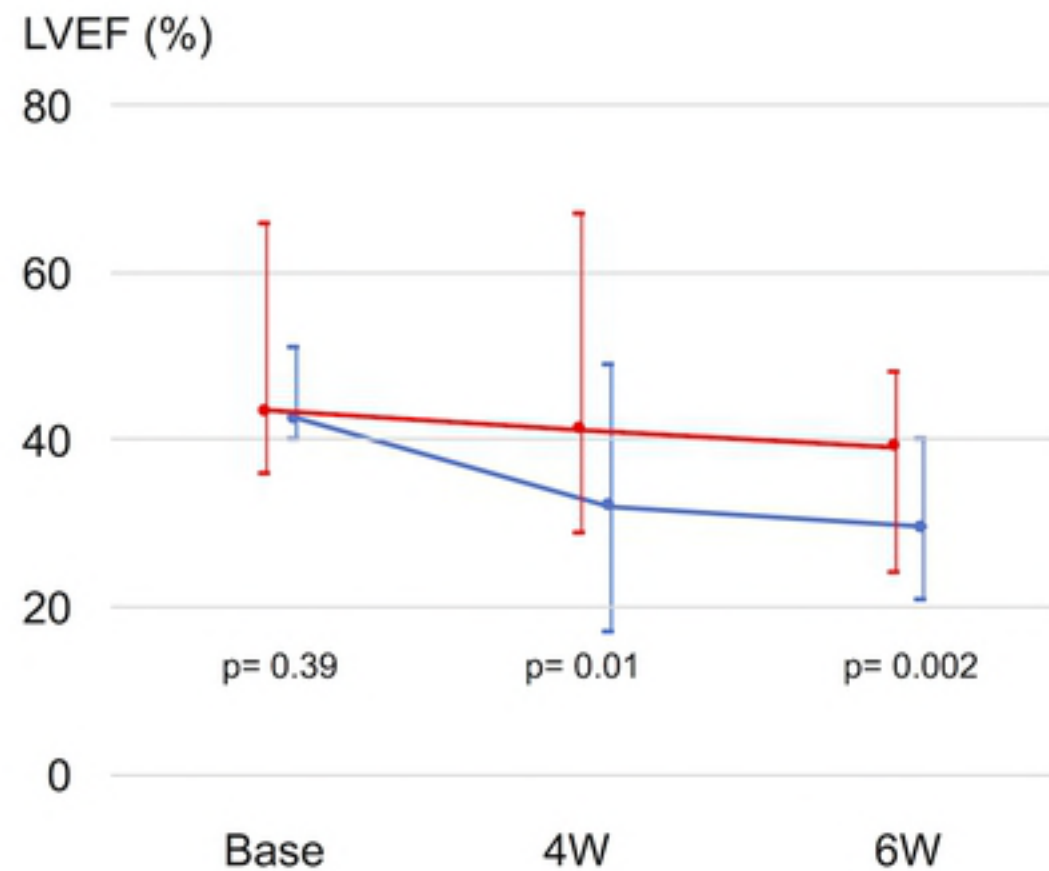
558 Reorganization of cytoskeletal proteins and prolonged life expectancy caused by hepatocyte

559 growth factor in a hamster model of late-phase dilated cardiomyopathy. J Thorac

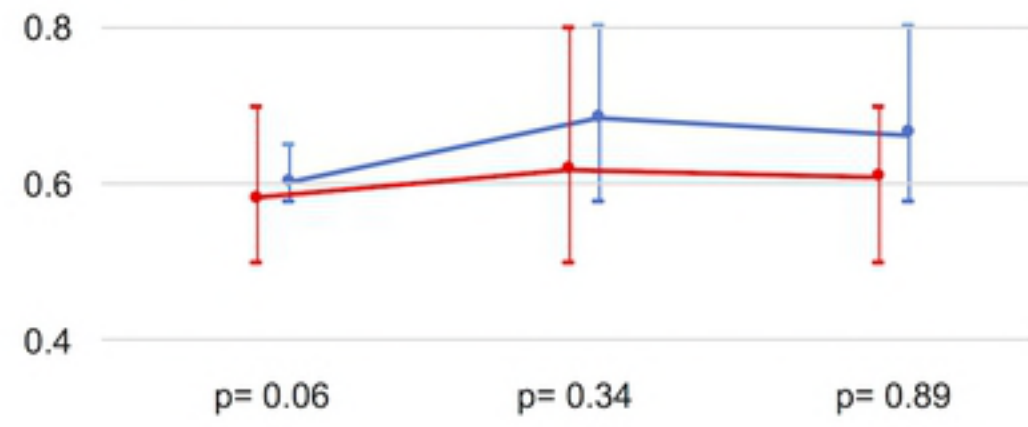
560 Cardiovasc Surg. 2005;130:295-302

561

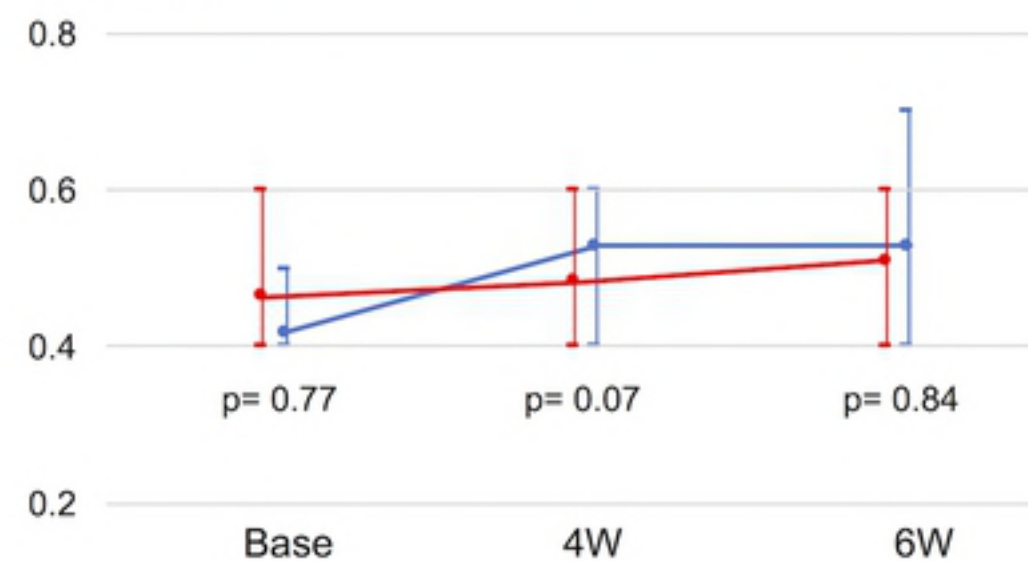
HMGB1 group
Control group

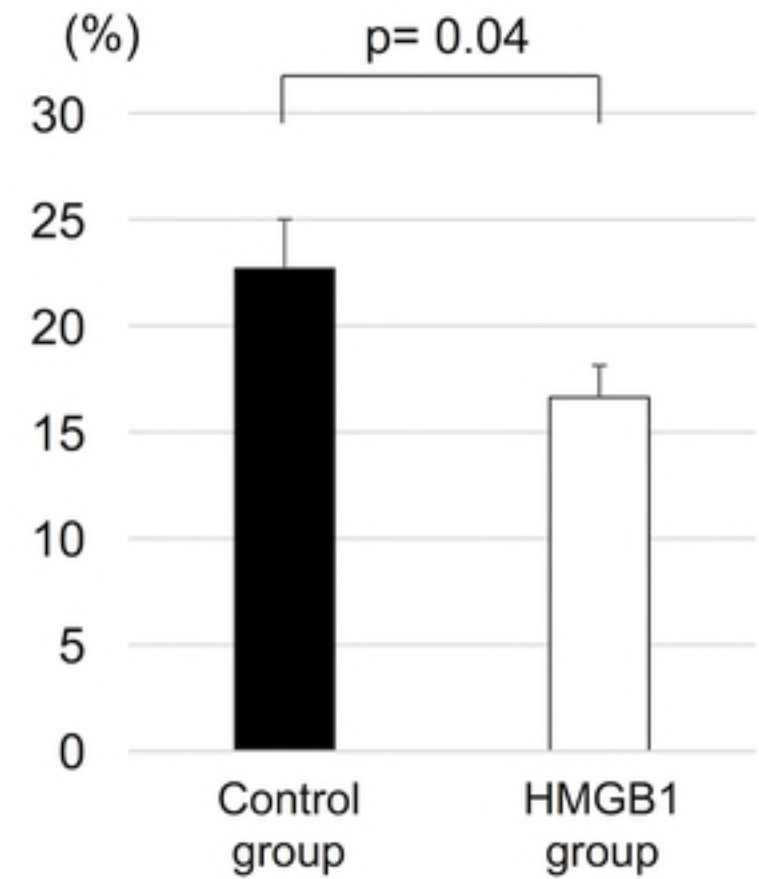
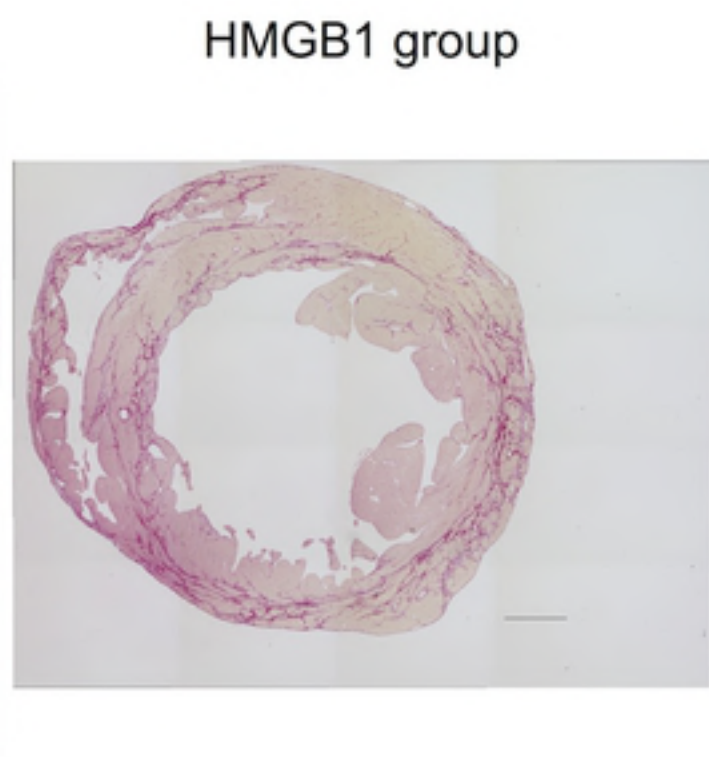
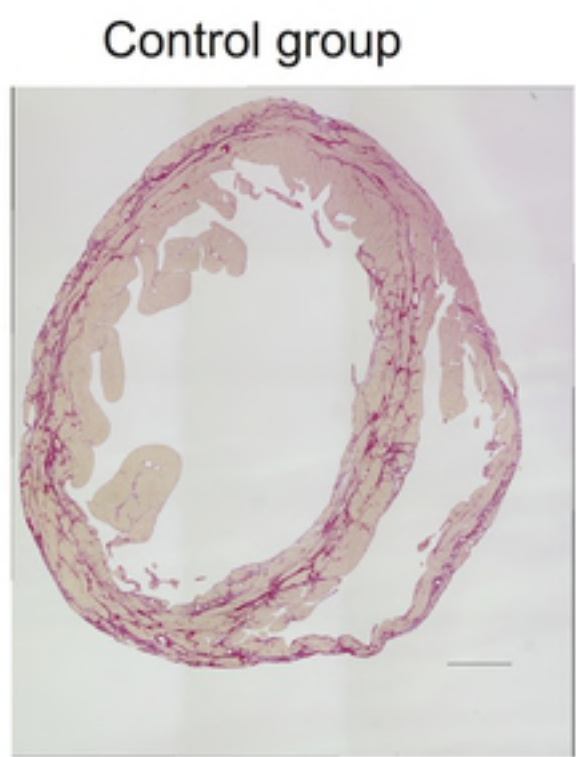


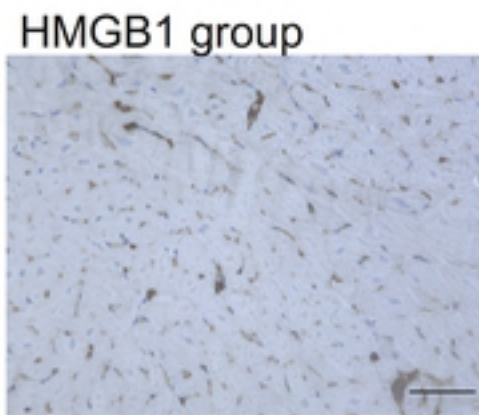
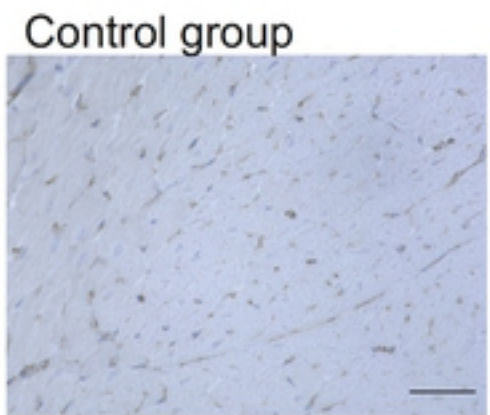
LVDd (mm)



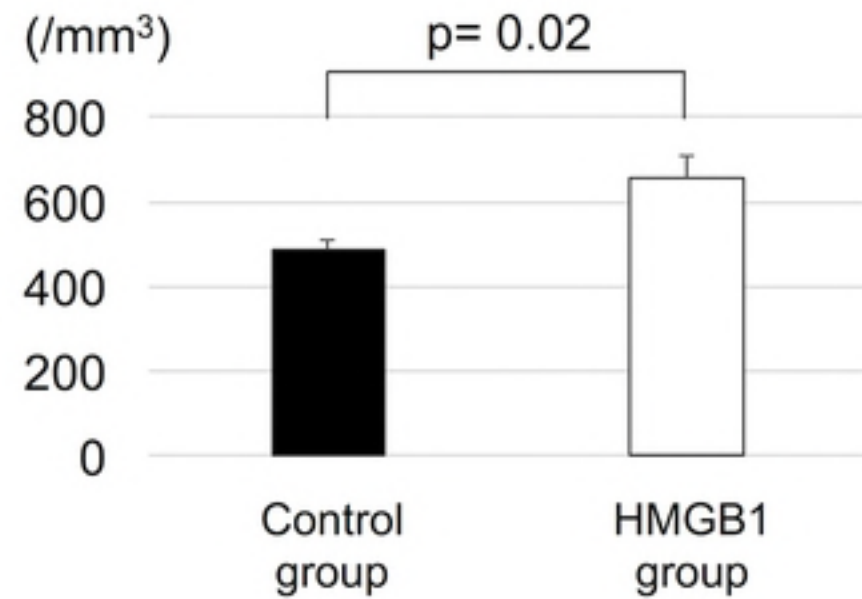
LVDs (mm)

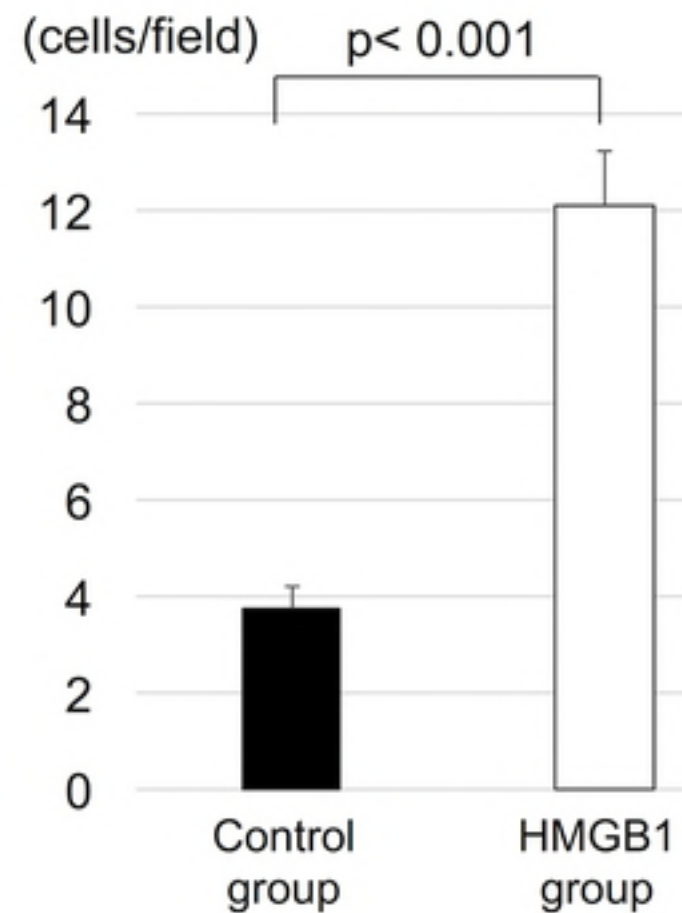
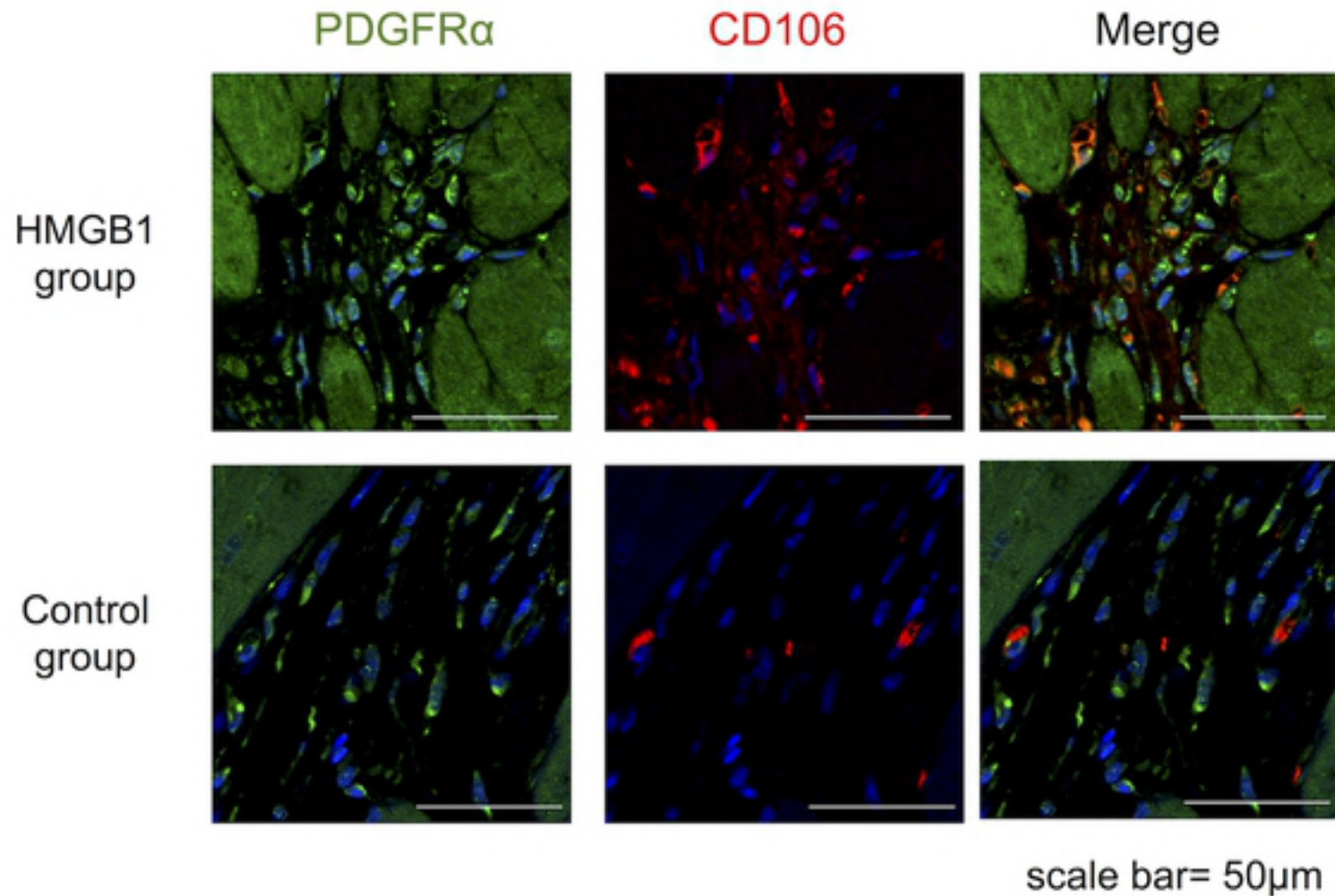


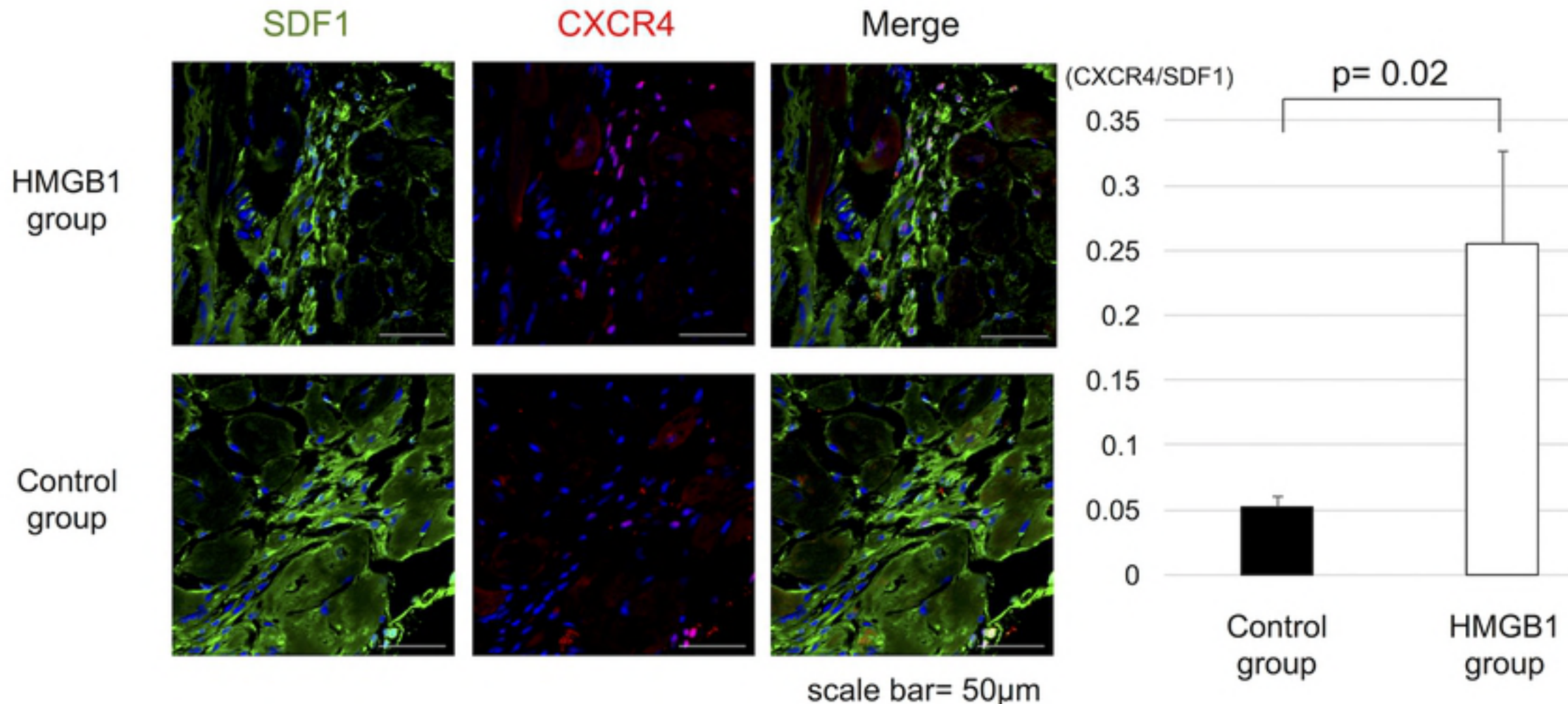




scale bar= 50 μ m

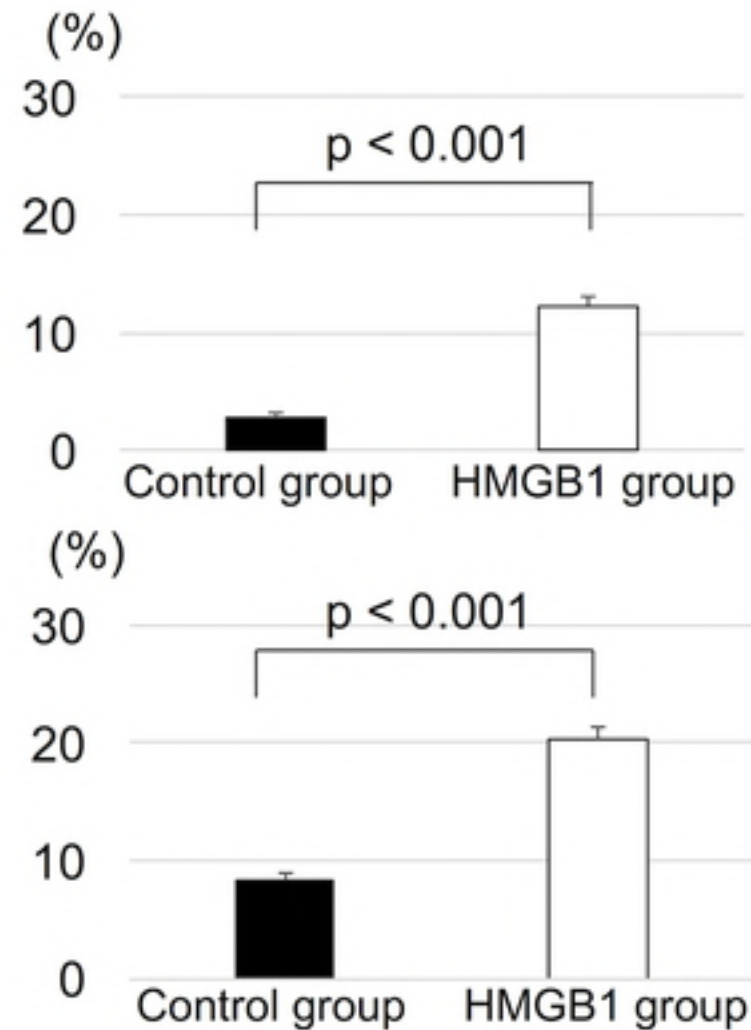
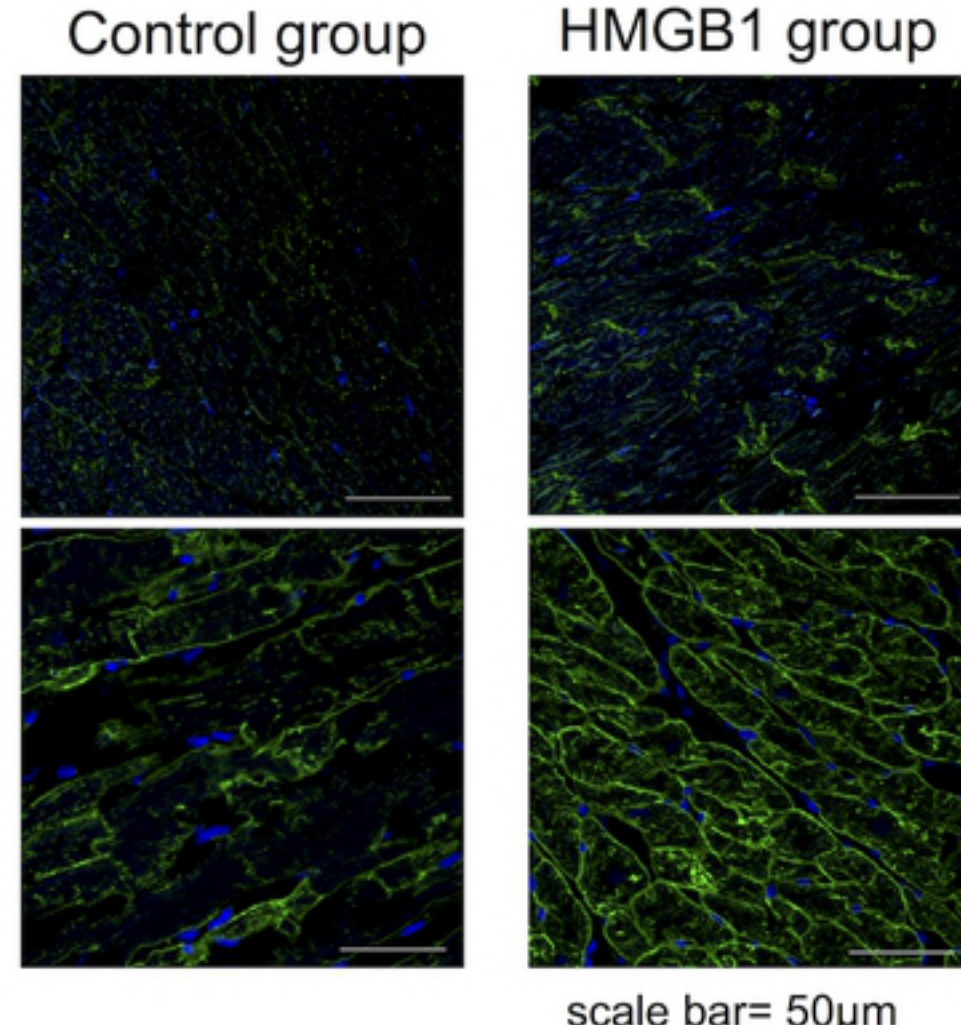


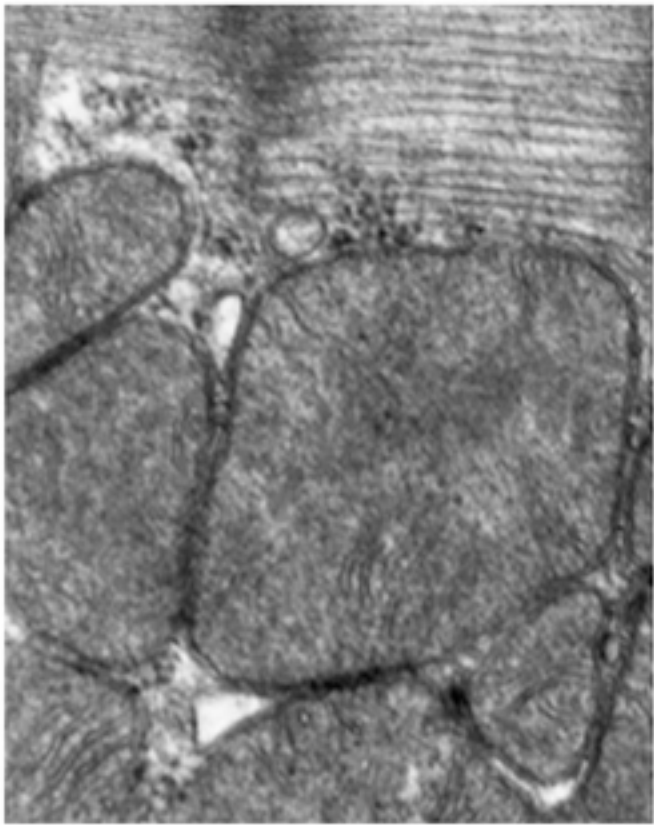




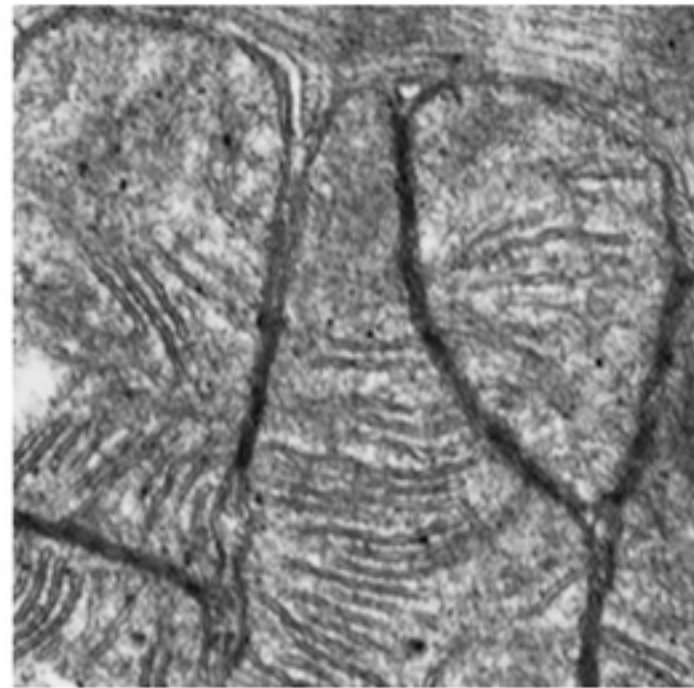
DAPI
 α -sarcoglycan

DAPI
 α -dystroglycan

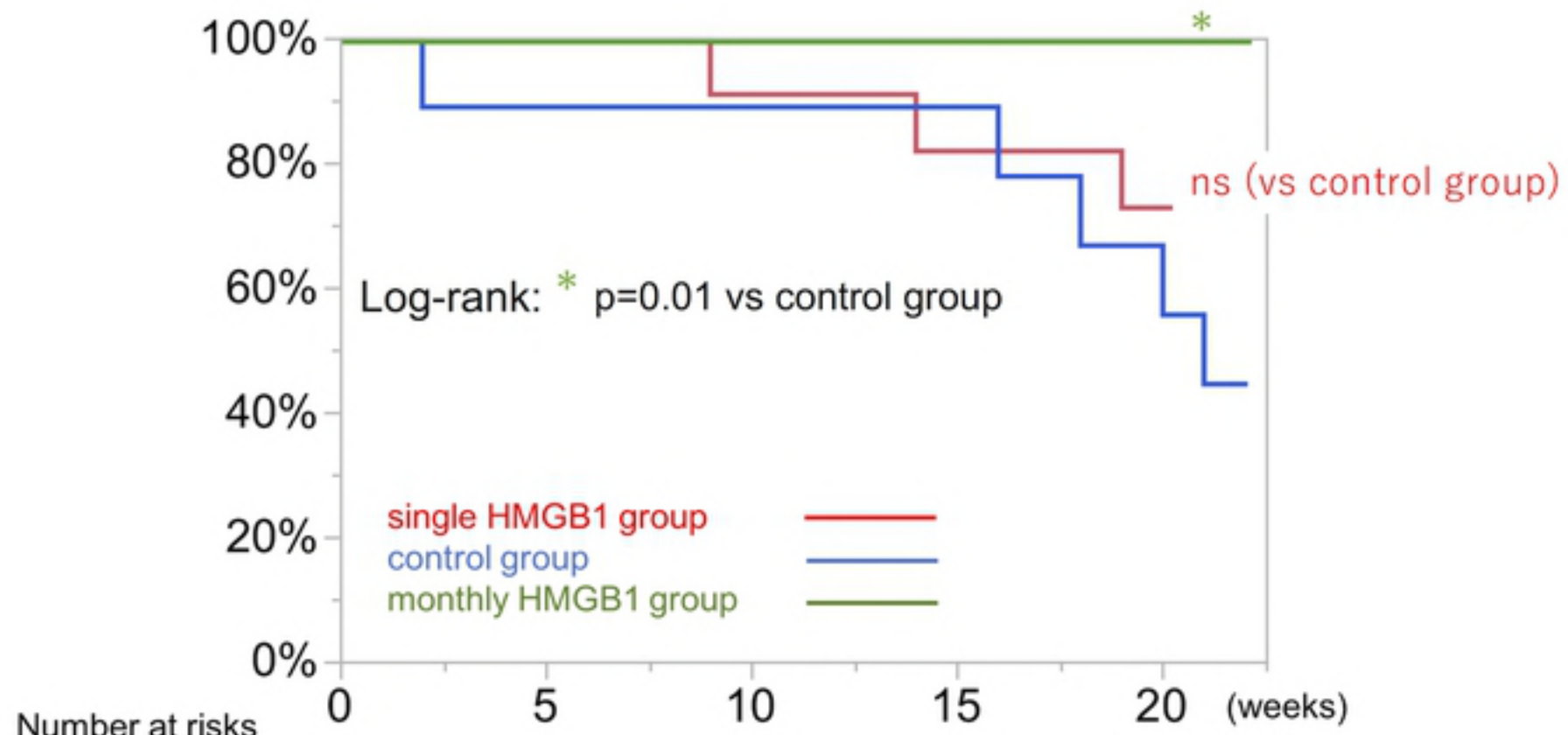




Control group



HMGB1 group



single HMGB1 group

11

10

9

8

control group

8

8

8

6

monthly HMGB1 group

9

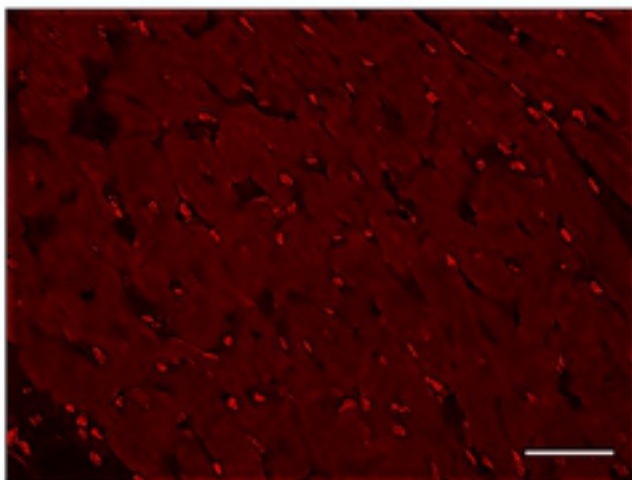
9

9

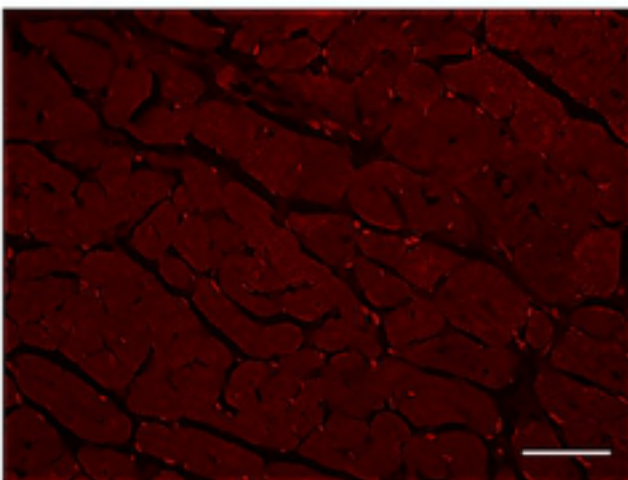
9

(a)

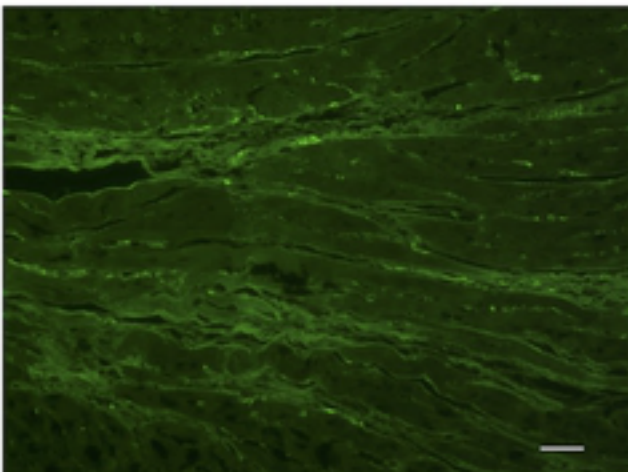
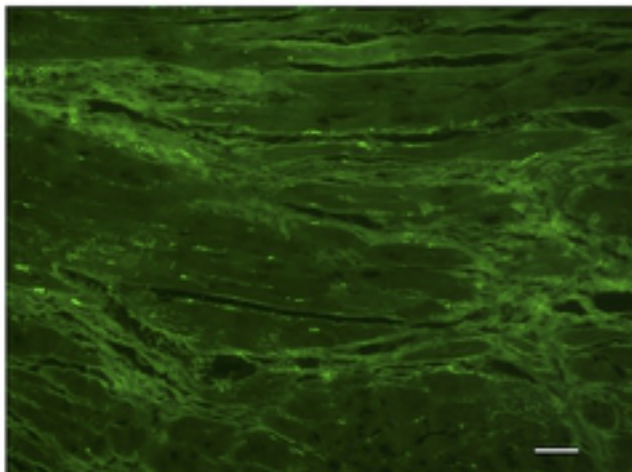
Control group



HMGB1 group



(b)

scale bar= 50 μ m

(c)

(/mm³)

1500

1000

500

0

p< 0.001

(d)

(%)

8

6

4

2

0

Control group HMGB1 group

p= 0.06



Control group HMGB1 group